



CHORUS

This is the accepted manuscript made available via CHORUS. The article has been published as:

Influence of spatial delay on the modulational instability in a composite system with a controllable nonlinearity

Monisha Kumar, K. Nithyanandan, and K. Porsezian

Phys. Rev. E **97**, 062208 — Published 18 June 2018

DOI: [10.1103/PhysRevE.97.062208](https://doi.org/10.1103/PhysRevE.97.062208)

Influence of spatial delay on the modulational instability study in a composite system with a controllable nonlinearity

Monisha Kumar¹, K. Nithyanandan^{2,3}, K. Porsezian^{*1}

¹*Department of Physics, School of Physical, Chemical and Applied Sciences,
Pondicherry University, Pondicherry 605014, India*

²*Laboratoire Interdisciplinaire Carnot de Bourgogne, UMR 6303 CNRS,*

Université de Bourgogne, 9 avenue A. Savary, BP 47870, Dijon Cedex F-21078, France.

³*CNRS/Université Joseph Fourier, Laboratoire Interdisciplinaire de Physique (LIPHY), Grenoble, France.*

**Email: ponzsol@gmail.com*

A theoretical investigation on the modulational instability (MI) in a composite system with non-local response function is presented. A composite system of silver nanoparticles in acetone is chosen, whose nonlinearity can be delicately varied by controlling the volume fraction of the constituents, thus enabling the possibility of nonlinearity management. A pump-probe counter propagation configuration has been assumed and the interplay between the competing nonlinearities and the non-localities in the MI dynamics is systematically explored. Different class of nonlocalities have been considered and the study reveals that the nonlocality critically depends on the kind of nonlocal function. However, the general behaviour is that the strength of nonlocality suppresses the MI gain, while for rectangular function it assists the emergence of new spectral windows. We also show that the cross coupling effects are significant in enhancing MI, especially in the defocusing nonlinearity. We also emphasize the impact of the relative strength of the nonlinearities in the MI dynamics at different settings of competing nonlinearities. Thus, we emphasize the importance of the different class of nonlocal response in the MI dynamics, and explored the interplay between the higher order nonlinear effects and nonlocalities in the counter propagating configurations.

PACS numbers: 42.65.Wi,42.65.Tg,42.65.-k,42.81.Dp

I. INTRODUCTION

Advancement in material chemistry and photonic technologies have opened new frontiers in research on plasmonics and nanophotonics. Of late, particularly, “composites” with interesting controllable physical properties played a vital role in the development of novel plasmonic applications. A composite is a material made from two or more constituent materials with distinct physical/chemical properties, that when combined produce a material with different characteristics from individual components. Commonly used composites are of two types (*i*) spatially separated metal nanoparticles embedded in a dielectric host and (*ii*) fractal aggregates of metal nanoparticles [1]. For systems containing metallic nanoparticle, the surface plasmon resonance (SPR) plays an important role, modifying, for instance, linear and nonlinear optical properties of the material [2, 3].

In the development of the novel materials aiming photonic applications, colloidal systems containing metal nanoparticles are very promising owing to the enhancements of the nonlinear absorption and nonlinear refractive index observed in such systems [4, 5]. These changes on the nonlinear optical properties of a colloid can be mainly attributed to two different origins: Local field effect and large nonlinear response of metals. Thermal properties of metal nanocomposites critically depend on the concentration of nanoparticles and play an important role in the determination of the colloid characteristics of the composite structure. For example,

it was found in a colloidal system of gold nanoparticles in castor oil, that, even though the laser wavelength was not resonant with the surface plasmon absorption band, significant enhancement of electronic and thermal nonlinearities were observed. The presence of nanoparticles enhanced both local (electronic) and nonlocal (thermal) nonlinear response of the colloids. The electronic part of the nonlinearity was enhanced by at least two orders of magnitude depending on the particle filling fraction. On the other hand the thermo-optical properties of the colloidal systems is rather more sensitive and changes dramatically as the filling fraction was increased [6].

During the last century or so, optical properties of nanoparticles have extensively been studied and metal-dielectric nanocomposites (MDNCs) have found various applications in different fields of science and technology. Since the optical properties of metal nanoparticles are typically governed by SPR, they are strongly dependent on the nanoparticles size, shape, concentration and spatial distribution as well as on the properties of the surrounding matrix. Control over these parameters enables such MDNC to become promising media for the development of novel non-linear materials, nanodevices and optical elements [7]. Especially, in the context of nonlinear plasmonics, the MDNCs are promising contenders and plays an indispensable role in realizing system endowed with nonlinearity management [8]. The emergence of nonlinear plasmonics has developed a renewed interest in the studies related to higher-order nonlinearities (HON). MDNC happened to be an ideal

candidate to serve the purpose of delicate management of nonlinearity by appropriate ratio of the volume fraction of nanoparticles to that of the host. This way of controlling the nonlinearity of the system is advantageous indeed, as it would enable “on demand” control on each order of nonlinear susceptibility in the system. For instance, by a proper choice of the volume fraction of nanoparticles, one can even nullify the cubic nonlinearity while the quintic or septimal nonlinearities can still be finite [9]. This enables one to tailor-made the effective nonlinearity making MDNC as a potential choice for nonlinear management. In the recent past, competing nonlinearities also have drawn much attention. Such nonlinearities occur in media where a few different physical processes contribute to the overall nonlinear response. A few examples to mention are, Bose-Einstein condensates with simultaneous local and long range interactions [10] and nematic liquid crystals with comparable thermal and orientational nonlinearities [11].

Another interesting feature typical to the systems like MDNC is the nonlocal nonlinearity, meaning that the nonlinearity is a nonlocal function of the incident field. Even though there are a lot of studies on nonlocal nonlinearities in the soliton context, most of them are related to the studies on propagation in the fibers and BECs [12–14]. For instance, in the case of single dark spatial solitons, nonlocality tends to expand the width of the solitons. Spatial nonlocality provides stabilization of bright solitons and induces their attraction, even if they are out of phase and in case of dark solitons, attraction induced by nonlocality can lead to the formation of their band states and in case of vortices nonlocality can stabilize the vortex propagation [15].

One of the intriguing manifestation in the propagation dynamics of any nonlinear media is the so-called modulation instability (MI). MI is a nonlinear phenomenon, where a continuous wave (CW) or a quasi-CW undergoes a modulation of its amplitude or phase in the presence of noise or any other weak perturbations. The modulation process may eventually grow and lead to the breakdown of the wave into a train of short pulses or filaments. The phenomenon of MI has been studied in a wide variety of physical systems like fluid dynamics [16, 17], plasma physics [18, 19], nonlinear fiber optics [20], Bose-Einstein Condensates [21–23], liquid crystals [24–26], and also in various plasmonic systems [27–29]. It has been shown that MI is strongly affected by various mechanisms in the nonlinear system [30–33], and in particular, the nonlocality in nonlinear response [34, 35] is one another intriguing effect that plays a substantial role in the dynamics of the system.

Recently, Reyna *et al* reported an experimental study on a composite system made up of silver nanoparticles suspended in acetone. In this important work, the

authors successfully realized a composite system with flexible nonlinearity management where the effective Kerr nonlinearity can be controlled at will, by merely changing the volume fraction of the silver nanoparticles. Through this way, they demonstrated different aspects of nonlinearity management and one interesting case would be the zero cubic nonlinearity with finite quintic nonlinearity. Indeed, this particular case is interesting, as it is not possible in the conventional system. In a similar context, they also studied the dynamics of spatial MI at different settings in the limit of effective local nonlinear response. In principle, in composite systems as in Ref.[36], the nonlinearity is not strictly local and the effective nonlinearity is a nonlocal function of the incident field. This is particularly true because of the strong confinement of electric field due to the formation of plasmonic modes in metal nanoparticles, which can enhance the nonlinear effects whose strength crucially depends on the particular function of nonlocality. Therefore in order to accurately model the dynamics, one has to incorporate the nonlocality in the nonlinear response. Of late, there had been a few studies on MI in nonlocal nonlinear media. To mention a few includes, Krolikowski *et al* has studied MI in nonlocal nonlinear Kerr media with different kind of nonlocalities like weak, strong and general nonlocal effects [37]. Wang *et al* has studied MI in nonlocal Kerr media with sine-oscillatory response[38]. Tiofack *et al* has studied the effect of competing cubic-quintic nonlinearities on MI in non-Kerr type media showing equal nonlocal response functions [39], also MI in media with a local quintic and a nonlocal cubic nonlinearities was studied in Ref. [40].

Most cases of nonlocal MI studies are primarily based on single optical beam and such kind of MI is termed as scalar MI. The co-propagation(or counter-propagation) of two or more optical beams can lead to interesting and peculiar phenomena which could not be realized in the single beam case [41, 42]. As a matter of fact, one of the breakthroughs in MI is the realization of MI in normal dispersion (or diffraction) regime. [41]. As it is known the normal group velocity dispersion (GVD) regime is not subject to the MI process, due to the lack of phase matching between the dispersion and nonlinear components of the system. But the nonlinear coupling between the two co-propagating beams due to the cross-phase modulation (XPM) (i.e., refractive index seen by one wave depends on the intensity of the co-propagating wave through the XPM coefficient) destabilize the steady state leading to frequency modulation even in the normal GVD regime [41, 42]. These interesting results set the benchmark for the extensive work on two-color light propagation in the optical system.

Motivated by the interesting nonlinear properties associated with the composite structure, and the physical importance of coupled nonlinear system in MI process, in what follows, we study the XPM induced spatial MI in

a composite system with a nonlocal nonlinear response. Taking the advantage of the recent experimentally realized composite system made up of silver nanoparticles suspended in acetone by Reyna *et al*, our study focus on the coupled system in the same settings, with particular emphasize on the different functional form of nonlinear responses. The paper is organized as follows: section 2 describes the theoretical model and the propagation equation. In Section 3 we have applied linear stability analysis followed by the study of modulation instability with various nonlocal response functions for different competing nonlinearities in section 4. Further section 5 includes the conclusions.

II. THEORETICAL MODEL

The counter propagation of pump-probe beams in the composite medium is governed by the modified coupled nonlinear Schrodinger equation (CNLSE) of the form

$$\begin{aligned} & (-1)^j i \frac{\partial A_j}{\partial \xi} + \frac{1}{2} \frac{\partial^2 A_j}{\partial \rho^2} + \alpha_1 (|A_j|^2 + 2|A_{3-j}|^2) A_j \\ & + \alpha_2 (|A_j|^4 + 6|A_j|^2 |A_{3-j}|^2 + 3|A_{3-j}|^4) A_j = 0. \end{aligned} \quad (1)$$

where A_j with $j=1,2$ is the amplitude of the pump and probe beams in the composite medium respectively. Here the spatial coordinates have been normalized to $K^{-1} = \frac{\lambda}{2\pi n_0}$, where n_0 is the linear refractive index of the host medium and λ is the wavelength of the laser pump. ξ is the dimensionless direction of propagation which is defined as $\xi = zK$ and the dimensionless transverse coordinate ρ is given by $\rho = xK$. α_1 and α_2 are the strengths of the competing cubic and quintic nonlinearities respectively and it take positive (negative) sign for self-focusing (defocusing) nonlinearities.

Reyna *et al* proposed this model for light propagation in MDNC and studied the nonlinearity management and spatial modulation instability for cubic quintic nonlinearity [36], the two dimensional solitons for a quintic septimal medium [9] and the spatial phase modulation in the medium with quintic septic nonlinearity [43]. The theoretical model was developed using the generalized Maxwell-Garnet model under the assumption of a homogenous, isotropic medium with the nanoparticles uniformly distributed. The particle size a is smaller than the interparticle distance b which is smaller than the incident light wavelength λ .

Spatial nonlocality comes into the picture when the nonlinear refractive index at a given point is determined not only by the light intensity at that point but also by the intensity near that point. A phenomenological generic form of nonlocal nonlinear response induced by an optical beam of intensity $I(\rho, \xi)$ [37] is given by

$$\Delta n(I) = S \int_{-\infty}^{\infty} R(\rho - \rho') I(\rho', \xi) d\rho' \quad (2)$$

where $\Delta n(I)$ is the intensity dependent change in refractive index of the medium and RHS gives a spatial convolution integral with $R(\rho)$ as the nonlocal response function, defining the nonlocal character of the nonlinearity and its width (compared to the spatial extent of the beam) determines the degree of nonlocality with S representing the strength and sign of the nonlinear contribution. In the limiting case of $R(\rho) = \delta(\rho)$ the Eq. (2) describes the local response [39, 44, 45]. Even though the nonlocality model mentioned by Eq. (2) is phenomenological, it very well describes the features of nonlocal media. Typical nonlocal systems involve media with transport processes as ballistic atomic transport or heat diffusion as in atomic vapours or charge transport in photorefractive crystals or charge separation in thermal media or plasma. Also long range interactions are responsible for nonlocal responses in liquid crystals or dipolar BECs [15, 46].

The coupled NLSE with the phenomenological generic model of competing nonlocal nonlinear responses is given by [36, 39]

$$\begin{aligned} & (-1)^j i \frac{\partial A_j}{\partial \xi} + \frac{1}{2} \frac{\partial^2 A_j}{\partial \rho^2} + \alpha_1 \int_{-\infty}^{\infty} R_1(\rho - \rho') (|A_j|^2 + \\ & 2|A_{3-j}|^2) A_j d\rho' + \alpha_2 \int_{-\infty}^{\infty} R_2(\rho - \rho') (|A_j|^4 + 6 \\ & |A_j|^2 |A_{3-j}|^2 + 3|A_{3-j}|^4) A_j d\rho' = 0; j = 1, 2; \end{aligned} \quad (3)$$

The model Eq (3) refers to the evolution of pump-probe pulses in the MDNC media where we have incorporated the phenomenological generic model of nonlocal response of nonlinearity. The response function $\int_{-\infty}^{\infty} R(\rho - \rho')$ shows the surrounding spatial region/range/domain of homogenous isotropic MDNC medium responding to the refractive index change due to the intense pump pulse intensity at a point ρ' in the medium. We take the intensity profile $I(\rho')$ and the width of the nonlocal response function $R(\rho - \rho')$ comparable, owing to the general nonlocal nonlinear response. **The cause of nonlocal nonlinear response in the composite can be due to the phenomenon of advection or the thermal nonlinearity due to the presence of metal nanoparticles as described by Souza et.al [6].** The nonlinear response of the composite medium is given by various nonlocal response functions. Here we study the influence of various response functions on MI for different cases of nonlocal nonlinearities. The functions can be conveniently put into two classes based on whether the spectrum corresponding to the function is positive definite or not. The exponential and Gaussian functions belongs to positive definite while rectangular and sine-oscillatory are not characterized by positive definite spectrum. For the detailed study of the MI phenomenon, we specifically use the Gaussian and the rectangular response functions as the two representative categories. The various response functions and their Fourier transforms are tabulated in Table 1 and graphically represented as a function of κ

vector in fig 1.

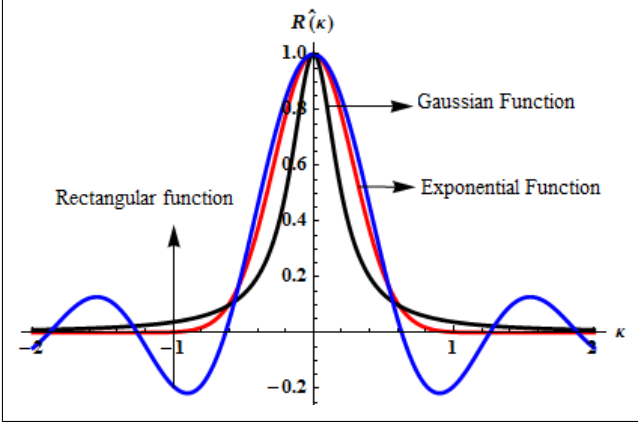


FIG. 1: (Color online) Various response functions in the κ space.

TABLE I: Various nonlocal response functions and there fourier transforms

function	$R(\rho)$	$\hat{R}(\kappa)$
Exponential	$\frac{1}{2\sigma} \exp(\frac{- \rho }{\sigma})$	$\frac{1}{1+\sigma^2\kappa^2}$
Gaussian	$\frac{1}{\sigma\sqrt{\pi}} \exp(\frac{-\rho^2}{\sigma^2})$	$\exp(\frac{-\sigma^2\kappa^2}{4})$
Rectangular	$\begin{cases} \frac{1}{2\sigma} & -\sigma \leq \rho \leq \sigma \\ 0 & \text{otherwise} \end{cases}$	$\frac{\sin(\kappa\sigma)}{\kappa\sigma}$
Sine - Oscillatory	$\frac{1}{2\sigma} \sin(\frac{ \rho }{\sigma})$	$\frac{1}{1-\sigma^2\kappa^2}$

III. LINEAR STABILITY ANALYSIS

The stability of the steady-state solution against small perturbation for the propagation equation is studied using linear stability analysis. To be more realistic, we assume the asymmetric plane wave solutions whose intensity of probe-pump beams are in the ratio 1:10 with a pump power of 31 KW and probe beam power of 3.1 KW [43]. The steady state solution of Eq. (3) is given by,

$$A_j(\rho, \xi) = \sqrt{P_j} \exp(i \phi_j \xi); j = 1, 2; \quad (4)$$

where P_j is the normalized pump and probe beam powers for $j=1,2$. Perturbing the plane wave solution in its amplitude with the complex perturbations and further linearizing, we get the model equation in terms of the

perturbations $a_j(\rho, \xi)$ and $a_{3-j}(\rho, \xi)$ as,

$$\begin{aligned} & \int_{-\infty}^{\infty} \sqrt{P_j} (2a_{3-j}(\rho', \xi) \sqrt{P_{3-j}} (r_1 \alpha_1 + 3(P_j + P_{3-j}) r_2 \alpha_2) \\ & + a_j(\rho', \xi) \sqrt{P_j} (r_1 \alpha_1 + 2(P_j + 3P_{3-j}) r_2 \alpha_2) + \\ & \sqrt{P_j} (r_1 \alpha_1 + 2(P_j + 3P_{3-j}) r_2 \alpha_2) a_j^*(\rho', \xi) + \\ & 2\sqrt{P_{3-j}} (r_1 \alpha_1 + 3(P_j + P_{3-j}) r_2 \alpha_2) a_{3-j}^*(\rho', \xi)) d\rho' + \\ & \frac{1}{2} \frac{\partial^2 a_j(\rho, \xi)}{\partial \rho^2} + (-1)^j i \frac{\partial a_j(\rho, \xi)}{\partial \xi} = 0; \quad (5) \end{aligned}$$

where $r_1 = R_1(\rho - \rho')$ and $r_2 = R_2(\rho - \rho')$. We assume the following form of perturbation

$$a_j(\rho, \xi) = a_{j1}(\rho, \xi) + i a_{j2}(\rho, \xi); j = 1, 2; \quad (6)$$

where $a_{j1}(\rho, \xi)$ and $a_{j2}(\rho, \xi)$ are the real and the imaginary parts of the perturbation with $a_j^*(\rho, \xi)$ as its complex conjugate. Substituting Eq (6) into Eq (5) and separating the real and imaginary parts from the linearized equation, we get,

$$\begin{aligned} & \frac{\partial a_{j1}(\rho, \xi)}{\partial \xi} + \frac{(-1)^j}{2} \frac{\partial^2 a_{j2}(\rho, \xi)}{\partial \rho^2} = 0, \\ & \int_{-\infty}^{\infty} ((2P_j r_1 \alpha_1 + 2(P_j + 3P_{3-j}) r_2 \alpha_2) a_{j1}(\rho', \xi) + \\ & 4\sqrt{P_j} \sqrt{P_{3-j}} (r_1 \alpha_1 + 3(P_j + P_{3-j}) r_2 \alpha_2) a_{(3-j)1}(\rho', \xi)) d\rho' + \\ & (-1)^{j+1} \frac{\partial a_{j2}(\rho, \xi)}{\partial \xi} + \frac{1}{2} \frac{\partial^2 a_{j1}(\rho, \xi)}{\partial \rho^2} = 0; j = 1, 2; \quad (7) \end{aligned}$$

Applying the convolution theorem and using the Fourier transform [37] of the following form,

$$\begin{aligned} \hat{a}_j(\kappa, \xi) &= \int_{-\infty}^{\infty} a_j(\rho, \xi) e^{i\kappa\rho} d\rho, \\ \hat{R}(\kappa) &= \int_{-\infty}^{\infty} R(\rho) e^{i\kappa\rho} d\rho. \quad (8) \end{aligned}$$

We have the set of four differential equations as follows,

$$\begin{aligned} & \frac{\partial \hat{a}_{j1}}{\partial \xi} + (-1)^j \frac{(i\kappa)^2}{2} \frac{\partial \hat{a}_{j2}}{\partial \rho^2} = 0 \\ & 2P_1 (\hat{R}_1 \alpha_1 + 2(P_j + 3P_{3-j}) \hat{R}_2 \alpha_2) \hat{a}_{j1} + \\ & 4\sqrt{P_j} \sqrt{P_{3-j}} (\hat{R}_1 \alpha_1 + 3(P_j + P_{3-j}) \hat{R}_2 \alpha_2) \hat{a}_{(3-j)1} \\ & + (-1)^{j+1} \frac{\partial \hat{a}_{j2}(\rho, \xi)}{\partial \xi} + \frac{(i\kappa)^2}{2} \frac{\partial^2 \hat{a}_{j1}}{\partial \rho^2} = 0; j = 1, 2; \quad (9) \end{aligned}$$

The coefficient matrix of the above equation can be obtained as;

$$\begin{pmatrix} 0 & -\frac{\kappa^2}{2} & 0 & 0 \\ \mathbf{m}_1 & 0 & -\mathbf{m}_2 & 0 \\ 0 & 0 & 0 & \frac{\kappa^2}{2} \\ \mathbf{m}_2 & 0 & \mathbf{m}_3 & 0 \end{pmatrix}$$

where,

$$\begin{aligned}\mathbf{m}_1 &= \frac{1}{2}(\kappa^2 - 4P_1\hat{R}_1\alpha_1 - 8P_1(P_1 + 3P_2)\hat{R}_2\alpha_2) \\ \mathbf{m}_2 &= 4\sqrt{P_1}\sqrt{P_2}(\hat{R}_1\alpha_1 + 3(P_1 + P_2)\hat{R}_2\alpha_2) \\ \mathbf{m}_3 &= \frac{1}{2}(-\kappa^2 + 4P_2\hat{R}_1\alpha_1 + 8P_2(3P_1 + P_2)\hat{R}_2\alpha_2)\end{aligned}$$

We consider λ as the eigen value of the above matrix and one can write the characteristic equation of the above matrix as

$$|A - \lambda I| = 0 \quad (10)$$

Hence the eigen value λ [37] of the coefficient matrix is given by

$$\lambda = \pm \frac{1}{2}\sqrt{\lambda_a \pm \lambda_b}; \quad (11)$$

where

$$\begin{aligned}\lambda_a &= (-\kappa^4 + 2\kappa^2 P_2 \hat{R}_1 \alpha_1 + 4\kappa^2 P_1^2 \hat{R}_2 \alpha_2 + 4\kappa^2 P_2^2 \hat{R}_2 \alpha_2 \\ &\quad + 2\kappa^2 P_1 (\hat{R}_1 \alpha_1 + 12P_2 \hat{R}_2 \alpha_2));\end{aligned} \quad (12)$$

and

$$\begin{aligned}\lambda_b &= 2\kappa^2 \sqrt{(4P_1^4 \hat{R}_2^2 \alpha_2^2 + P_2^2 (\hat{R}_1 \alpha_1 + 2P_2 \hat{R}_2 \alpha_2)^2 + 4P_1^3 \hat{R}_2 \alpha_2 \\ &\quad (\hat{R}_1 \alpha_1 + 36P_2 \hat{R}_2 \alpha_2) + 2P_1 P_2 (7\hat{R}_1^2 \alpha_1^2 + 46P_2 \hat{R}_1 \hat{R}_2 \alpha_1 \alpha_2 + \\ &\quad 72P_2^2 \hat{R}_2^2 \alpha_2^2) + P_1^2 (\hat{R}_1^2 \alpha_1^2 + 92P_2 \hat{R}_1 \hat{R}_2 \alpha_1 \alpha_2 + 280P_2^2 \hat{R}_2^2 \alpha_2^2))};\end{aligned} \quad (13)$$

Hence λ has 4 different values. The MI gain is given by

$$G(\kappa) = \text{Re } \lambda \quad (14)$$

We note that MI is possible only for the eigen value $\lambda = \pm \frac{1}{2}\sqrt{\lambda_a + \lambda_b}$ where both λ_a and λ_b are real for the condition $4\hat{R}_2^2 \alpha_2^2 (P_1^4 + P_2^4 + 36P_1^3 P_2 + 36P_2^2 + 70P_1^2 P_2^2) + \hat{R}_1^2 \alpha_1^2 (P_2^2 + 14P_1 P_2 + P_1^2) > 4(P_2^2 + P_1^3 + 23P_1^2 P_2) \hat{R}_1 \hat{R}_2 \alpha_1 \alpha_2$. The spatial frequency corresponding to the maximum MI gain gives the optimum modulation frequency which is given by

$$\frac{dG(\kappa)}{d\kappa} = 0 \quad (15)$$

IV. MODULATIONAL INSTABILITY

As described earlier, one of the most sought feature of the composite system is its ability to tailor the effective nonlinearity of the system, which can enable one to naively control the plasmonic effect of the system. By assuming different combination of cubic and quintic nonlinearity in the regime of non-local response, we study various features of MI. In similar lines to the studies on MI, we first

study the effect of power on MI due to non-local nonlinearity. Further keeping the cubic nonlinearity constant, we vary the coefficient of the quintic nonlinearity and study the role of non-local responses on MI for various combination of nonlinearities and strength of nonlocalities. We also consider an intriguing special case relevant to composite system, where the cubic nonlinearity of the composite is null, while the effective nonlinearity can take finite values. For uniformity, we have used dotted lines to represent the rectangular response function and solid lines to represent Gaussian response function.

A. Effect of power

To start with, it is customary to understand the influence of pump power on MI for different kinds of nonlinear response functions. We have considered three representative combination of powers composing both symmetric and asymmetric solutions. (i) $P_1 = 1$, $P_2 = 0.1$ and (ii) $P_1 = 4$, $P_2 = 0.4$ are the choice of powers for asymmetric case, while (iii) $P_1 = 1$, $P_2 = 1$ corresponds to symmetric solution. We have plotted the Gaussian and the rectangular response functions separately with the nonlinear coefficients as $\alpha_1 = 1$ and $\alpha_2 = 0.1$ in Fig2(a) and 2(b), respectively. It is noted from Fig2(a) and Fig2(b) that MI gain increases with power for both the response functions as expected. The rectangular response function showed increase in the MI gain and number of bands with power. For Gaussian response function, MI gain increases with power for all cases of nonlinearities. In Fig2(c), where we have considered Gaussian response function with symmetric power and the strength of nonlinearities as $\alpha_1 = 1$ and $\alpha_2 = -0.1$ an anomaly noted is, here MI gain decreases for $P_1 = P_2 = 1$ to $P_1 = P_2 = 2$. At a power of 2 there is absolutely no MI and a further increase in power increases the MI gain. Apart from this, the symmetric solution in particular doesn't have any distinguished effect on MI from the asymmetric solution. Hence for the further discussions, we consider only the asymmetric solutions.

B. Effect of non-local strength

As the nonlocality play a crucial role in the dynamics of MI, in Fig. 3 we show the contour Map of MI spectra as a function of nonlocal strength. A general behaviour noticeable in the MI spectrum is that, the nonlocal strength monotonously decreases both the gain and bandwidth of the MI bands Fig. 3(a) and 3(b). Thus the nonlocal effect suppresses the MI. Interestingly, the rectangular response function show additional sidebands at higher κ , whose gain show unusual increase with σ as shown in the Fig. 3(b). The MI features due to different non-local response would be highlighted and comprehensively analyzed at different settings of nonlinearity in the following sections.

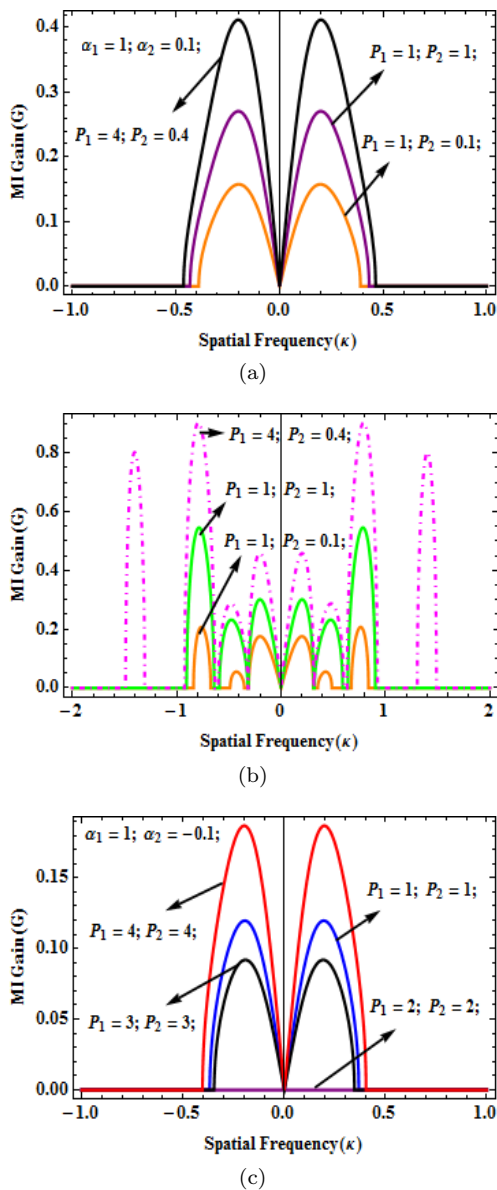


FIG. 2: (Color online) The variation of MI gain spectra with power for the focusing nonlinearity with (a) gaussian response function and (b) rectangular response function varying power as $P_1 = 1, P_2 = 0.1$; $P_1 = 1, P_2 = 1$ and $P_1 = 4, P_2 = 0.4$ and the strength of nonlocality is $\sigma = 10$ and the strength of nonlinearity as: (a) $\alpha_1 = 1, \alpha_2 = 0.1$ (b) $\alpha_1 = 1, \alpha_2 = 0.1$ (c) $\alpha_1 = 1, \alpha_2 = -0.1$ and the power varying symmetrically as $P_1 = P_2 = 1, 2, 3$ and 4 for the Gaussian response function.

C. MI at different settings of nonlinear response

The study of MI in the regime of higher order nonlinearity (HON) is interesting as it would lead to many new features, which would otherwise be impossible in the conventional system only with cubic nonlinearity. For instance, the quintic nonlinearity can either enhance or suppress MI and also at some parametric conditions can promote new sidebands. In what follows, we consider

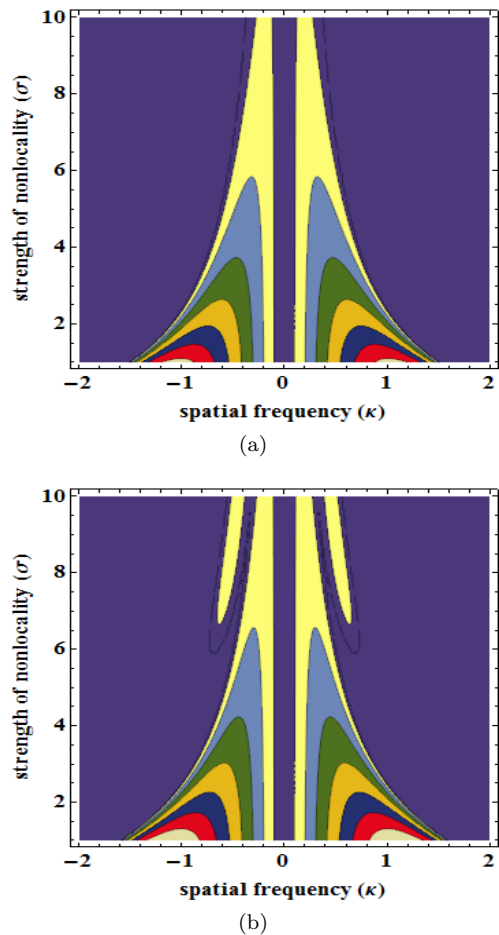


FIG. 3: (Color online) The MI gain spectra as a function of strength of nonlocality for the (a) Gaussian response (b) rectangular response for $P_1 = 1, P_2 = 1$ and $\alpha_1 = 1, \alpha_2 = -0.1$

three different regime of nonlinearity based on the sign of cubic nonlinearity and study MI with a particular emphasize on the non-local nonlinear response and quintic nonlinearity.

1. Focusing nonlinearity ($\alpha_1 > 0$)

This is a typical case of spatial MI, where MI is generally possible owing to the phase matching between the positive nonlinearity and diffraction. Two distinct types of non-local response namely, Gaussian and rectangular response function have been considered and the MI is studied for different combination of cubic and quintic nonlinearities as portrayed in Fig 4. With proper understanding of the effect of non-local strength from the previous section, to highlight other interesting features due to interplay between HON and non-locality, we choose two representative values of $\sigma = 5$ and 10 . Fig. 4(a) represent the case of $\alpha_1 > 0$ and $\alpha_2 > 0$, where both nonlinear

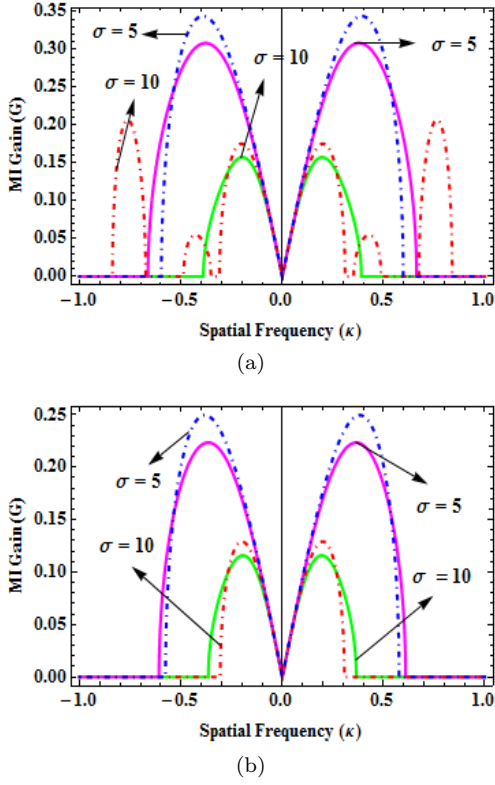


FIG. 4: (Color online) The MI gain spectra for the focussing nonlinearity with different nonlocal response function and varying the strength of nonlocality as $\sigma = 5, 10$ and the strength of nonlinearity as: (a) $\alpha_1 = 1, \alpha_2 = 0.1$ (b) $\alpha_1 = 1, \alpha_2 = -0.1$ with other parameters as $P_1 = 1$ and $P_2 = 0.1$

effects constructively reinforce to cause MI through phase matching with diffraction effects, as in the case of conventional scalar MI. This case is characterized by higher gain due to the enhancement of the effective nonlinearity as a result of the accumulated nonlinearity due to cubic and quintic effects. The rectangular function behaves qualitatively different leading to the emergence of new spectral sidebands which we refer as secondary bands. Whilst, the Gaussian response behaves quite similar to conventional MI. Fig. 4(b) corresponds to the case of $\alpha_1 > 0$ and $\alpha_2 < 0$, where both nonlinear effects compete due to its opposite sign and the resulting instability spectrum show MI bands with reduced gain, regardless of the nature of non-locality. In this case, both the Gaussian (solid line) and rectangular function behaves quite close, except the fact that the gain of primary band of the rectangular function is more, and conversely the bandwidth is lesser than the Gaussian function. It is also apparent from the Fig. 4, that the increase in the strength of the non-locality decreases the gain of MI, and in particular, new spectral bands originate for higher values of σ .

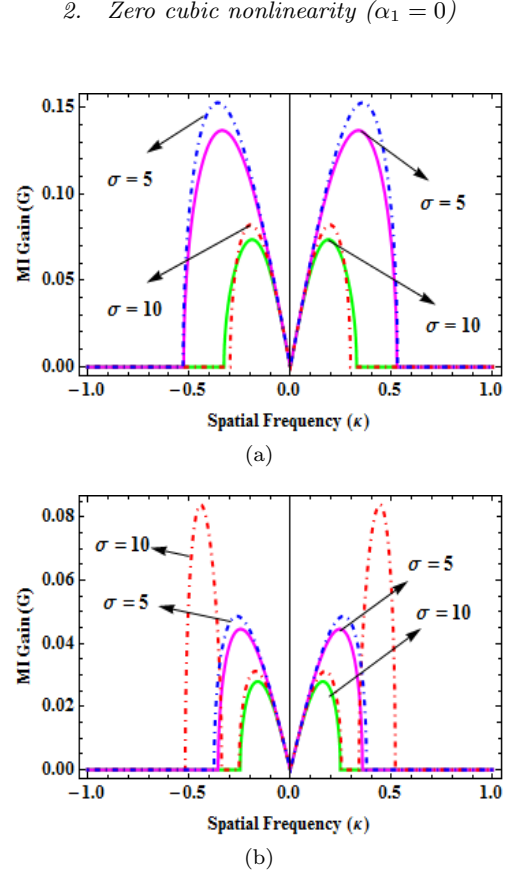


FIG. 5: (Color online) The MI gain spectra for the absence of cubic nonlinearity with varying the strength of nonlocality as $\sigma = 5, 10$ and the strength of nonlinearity as: (a) $\alpha_1 = 0, \alpha_2 = 0.1$ (b) $\alpha_1 = 0, \alpha_2 = -0.1$ with other parameter as $P_1 = 1$ and $P_2 = 0.1$

This is particularly an intriguing situation ($\alpha_1 = 0$ and $\alpha_2 \neq 0$) typically characteristic to the composite structures. Here, by proper choice of the volume fraction of the nanoparticles in the composite, one can delicately nullify the lower order nonlinear effects (cubic nonlinearity in the present setting), leaving only the next higher order effects to take control on the nonlinear effects of the system. Taking advantage of this unique feature, we consider different combination of quintic nonlinearity based on its sign. Fig. 5(a) represents the instability spectra for $\alpha_1 = 0$ and $\alpha_2 > 0$, where the much needed phase matching condition for the MI process is satisfied by the positive (focusing) quintic nonlinearity, a process quite similar to the conventional MI with cubic nonlinearity. Fig. 5(b) is the situation where the quintic nonlinearity takes negative value, still MI is made possible due to XPM effects because of the destabilization of steady state by XPM. It should be noted that, once the XPM effects are ignored this particular case is implausible for MI. In both the cases of quintic nonlinearity, the rectangular function dominates the gain, with additional sidebands for the case of $\alpha_2 < 0$. The effect of non-local strength in this case is rather interesting, such that the

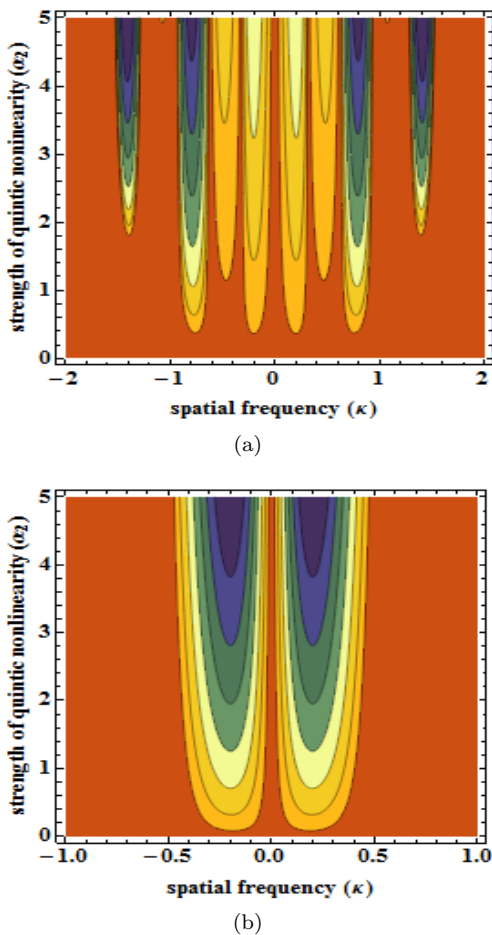


FIG. 6: (Color online) The MI gain spectra for the varying strength of quintic nonlinearity for the (a) rectangular and (b) gaussian response functions with the other parameters as $\sigma=10$, $\alpha_1=0$ $P_1=1$ and $P_2=0.1$

secondary spectral bands register a higher gain whose peak gain is more than twice the gain of the primary band. This is attributed to that fact the quintic nonlinearity generally promotes higher order spectral bands and with increase in the strength of the non-locality, both collectively acts to enhance the gain. As this case is particularly dominated by quintic nonlinearity, it is interesting to understand the strength of quintic nonlinearity in MI spectrum. Fig. 6 shows the evolution of spectral bands with strength of quintic nonlinearity for both the case of non-local functions. In both the cases, $|\alpha_2|$ enhance MI by increasing the gain of MI as well as the number of sidebands. Particularly, the effect of α_2 is more pronounced in rectangular function with additional spectral bands of higher gain (Fig. 6(a)), while the Gaussian function behaves rather in a straightforward way indicating monotonous increase of gain with α_2 as shown in Fig. 6(b).

3. Defocusing nonlinearity ($\alpha_1 < 0$)

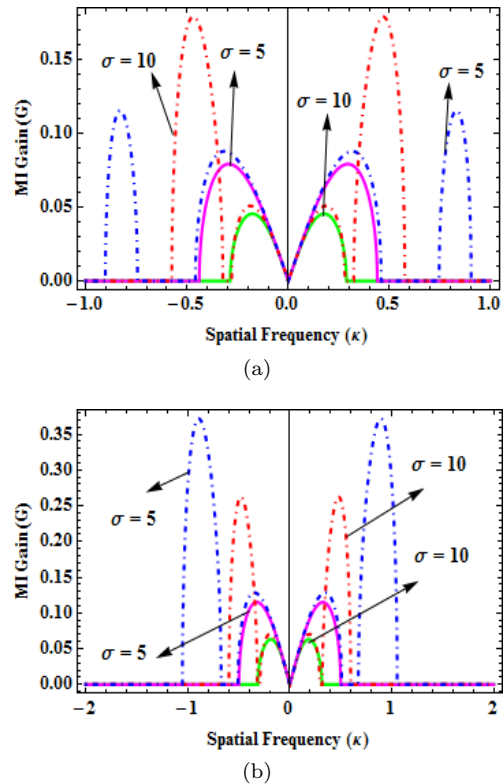


FIG. 7: (Color online) The MI gain spectra for the defocusing nonlinearity with different nonlocal response function and varying the strength of nonlocality as $\sigma=5, 10$ and the strength of nonlinearity as: (a) $\alpha_1 = -1, \alpha_2 = 0.1$ (b) $\alpha_1 = -1, \alpha_2 = -0.1$ and $P_1 = 1, P_2 = 0.1$

The defocusing nonlinearity is characterized by the negative values of the cubic nonlinearity and therefore, the MI can be realized either by virtue of quintic nonlinearity or through the XPM effects. Like in the previous section, two different combinations of cubic and quintic nonlinearity given by different signs of α_2 are considered. Fig. 7(a) represents the MI spectra corresponding to $\alpha_1 < 0$ and $\alpha_2 > 0$. In this case MI is possible by means of the focusing quintic nonlinearity and crucially depends on the relative strength of α_1 and α_2 , as both are in the opposite sign. One interesting feature of this particular case is the emergence of the additional sidebands even for lower value of σ for the rectangular response function. This emphasize the relevance of the quintic nonlinearity in the promotion of additional sidebands. Also, the relative secondary to primary peak gain is higher than the previous case of zero cubic nonlinearity. This quite clearly establish the constructive interplay between quintic nonlinearity and the non-local strength in the emergence of higher order sidebands. The Gaussian response shows a monotonous variation with strength of nonlocality as predicted in other cases. However the registered MI gain is lower than the focusing cubic nonlinearity, this is

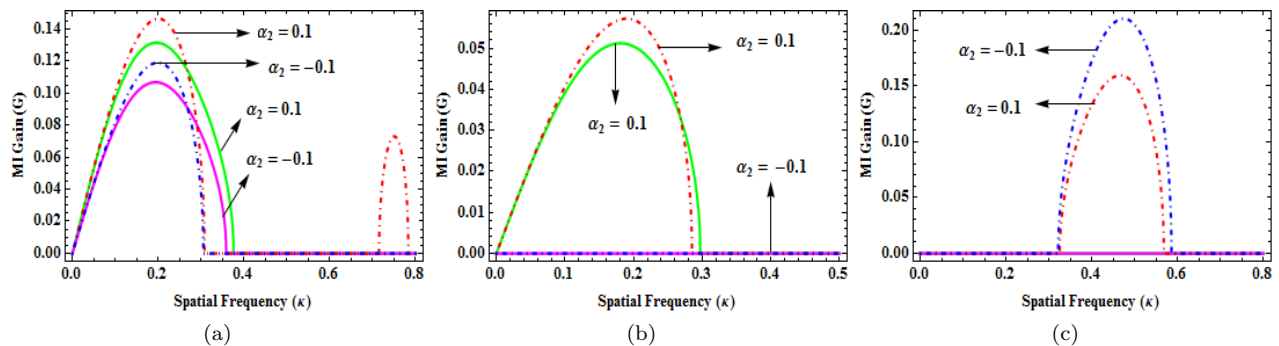


FIG. 8: (Color online) The MI gain spectra for the scalar NLS equation with the strength of nonlinearity as: (a) $\alpha_1=1$ (b) $\alpha_1=-1$ (c) $\alpha_1=-1$ and with other parameter as $P_1=1$, $P_2=0$, $\sigma=10$ and α_2 having values 0.1 and -0.1 in each case.

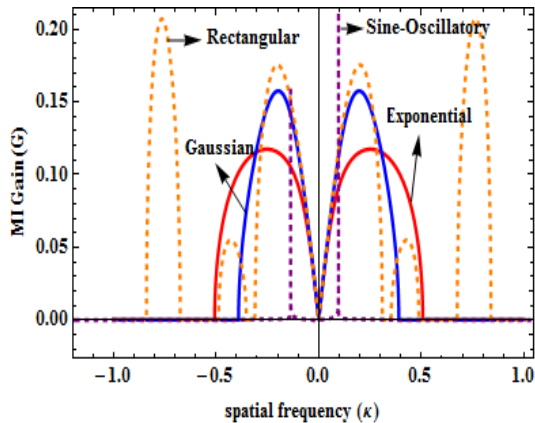


FIG. 9: (Color online) The MI gain spectra for different non-local response function with the various parameters as $\sigma=10$, $\alpha_1=1$, $\alpha_2=0.1$, $P_1=1$ and $P_2=0.1$.

clearly due to the weakened quintic nonlinearity of choice in this present case.

Fig. 7(b) is the case of $\alpha_1 < 0$ and $\alpha_2 < 0$ where both the nonlinearity are defocusing and the MI is realized purely by means of XPM effects and when the cross coupling effects are turned off, there is no instability in the case. So, XPM plays a critical role in the origin of MI in this regime. In this case, the nonlinearities only enhance the gain and not fundamental to the existence of instability. As in the previous case, the nonlocal strength decreases the MI gain, but for the choice of the parameters no higher order sidebands are noticed.

D. Results and Discussions

For a comprehensive picture and to make discussion self-explanatory, we reproduce some of the results corresponding to the scalar spatial MI [39, 40] and compare with the present results on counter-propagating coupled system. Fig. 8 show the MI spectra for three different cases of cubic nonlinearity as discussed before. As the

spectrum is symmetric $G(-\kappa) = G(\kappa)$, we content to show only the positive spectrum. To facilitate comparison with the previous discussion on counter propagating case, we ideally choose the same configuration of signs of α_1 and α_2 as before. Fig. 8(a) shows the MI of the focusing cubic media, where the solid line represents the Gaussian response, while dashed line is the case of rectangular nonlocal response. Two choice of quintic nonlinearity have been considered depending on the sign of α_2 . The Fig. 8(a) corresponds to the conventional

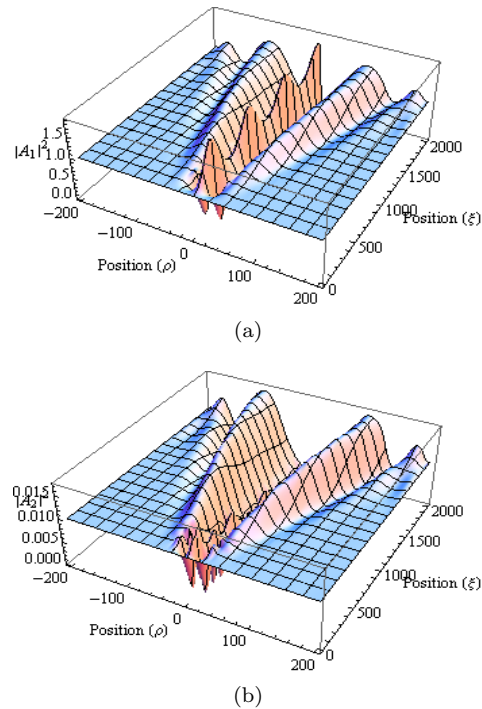


FIG. 10: (Color online) The direct simulation of the evolution of the (a) pump and the (b) probe beams with the the nonlocal response function as the gaussian function and the other parameters as $\alpha_1=0$, $\alpha_2=0.1$, $\sigma=10$, $A_{10}=1$, $A_{20}=0.1$ and $\omega_0=0.5$

MI, which has been studied extensively and an extensive

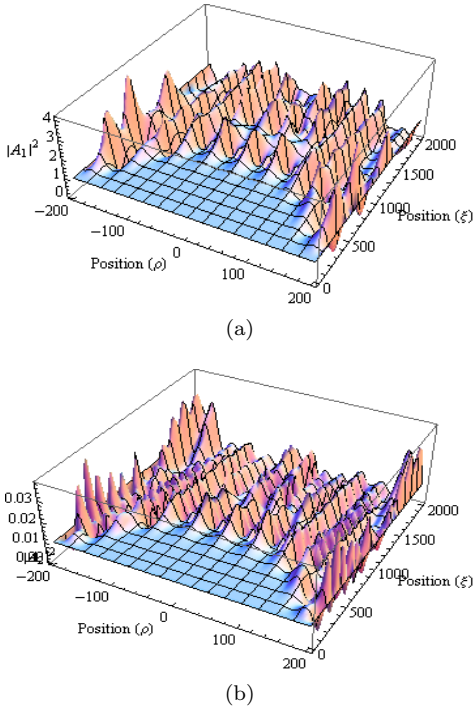


FIG. 11: (Color online) The direct simulation of the evolution of the (a) pump and the (b) probe beams with the non-local response function as the rectangular function and the other parameters as $\alpha_1 = 0, \alpha_2 = 0.1, \sigma = 10, A_{10} = 1, A_{20} = 0.1$ and $\omega_0 = 0.5$

discussion is needless here. It is apparent that the MI gain is significantly lower than the gain corresponding to Fig. 4, which agree with the results reported in the MI with local nonlinear response [42]. The case of zero cubic nonlinearity shown in Fig. 8(b) clearly show the absence of MI when $\alpha_2 < 0$, this is due to the lack of phase matching between diffraction and defocusing nonlinear effect. However, for the present problem on counter propagation case as described by the Fig.5, MI has been realized regardless of the sign of the quintic nonlinearity. The last is the case of defocusing cubic nonlinearity, in this case the origin of MI critically depends on the relative strength of α_1 and α_2 . Defocusing quintic nonlinearity(8(c)) is generally not feasible for MI, however for the case of rectangular non-local function, a secondary spectral band at higher κ is noted, while Gaussian function is not unstable and no MI is noticed. This observation is different from Fig. 7 of coupled system, where regardless of the combination of signs α_1 and α_2 the instabilities are inevitably noticed.

For the better insight and to give a global picture on the effect of various forms of popular nonlocal responses in the MI of composite system, we plot in the Fig. 9 the MI spectrum for different forms of available non-local functions. As discussed earlier, the various nonlocal functions are broadly classified into two classes, namely definite and indefinite positive spectrum. So far, our

whole study was based on a representative case of non-local functions from each categories, namely Gaussian and rectangular functions. It is quite evident that both class of nonlocal functions behaves qualitatively different, which is also evident from the Fig. 9.

The solid curve corresponds to exponential and Gaussian responses belonging to positive definite spectrum, where the behaviour of MI bands are similar to the local nonlinear system, difference being the magnitude of MI gain as a result of change in the effective nonlinearity. Whereas, the non-local response without positive definite spectrum such as rectangular and sine-oscillatory is infact interesting for MI, as it would lead to increased gain and additional instability window at higher κ as represented by dashed lines in the Fig. 9. The strength of nonlinearity also plays an important role, especially for the case of rectangular function, as new spectral spectral bands originates, which is found to be sensitive to σ (refer Fig.9).

Moreover, it should be noted that in-addition to the non-locality, the relative strength of the nonlinearity (α_1/α_2) and the cross coupling effects are decisive in the origin and the control of MI dynamics. For instance, there are cases like zero cubic and defocusing quintic nonlinearity (Fig. 5(b)) and defocusing cubic and quintic (Fig. 7(b)), the MI is attributed to the XPM effects, which destabilize the steady state solution to cause MI (refer Figs. 5(b) and 7(b)). While in the case of focusing quintic nonlinearity, regardless of the sign of cubic nonlinearity, the phase matching for MI is satisfied through defocusing quintic nonlinearity (Figs. 5(a) and 7(a)). Apart from XPM effects, the relative strength of nonlinearity play a substantial role in the emergence of additional sidebands in MI, which is particularly true for rectangular functions. It is noticed that depending on the value of the relative strength of nonlinearity, more number of additional bands are observed. Interestingly for zero cubic and defocusing cubic, for the parameter of choice, the MI gain of the secondary bands dominates, whose gain is nearly double than the conventional band.

For numerical appreciation, we numerically simulate Eq. 3 we choose the perturbed solution as, $A_1 = A_2 = A_{j0} + a_0 \cos(\omega_0 \rho)$, where A_{j0} is the amplitude of the propagating pump-probe beams and $a_0 = 10^{-4}$ is the small perturbation in the amplitude ω_0 is the optimum modulation frequency. $\xi = 2000$ is the dimensionless length of beam propagation, such that $z = \xi K^{-1}$ gives 0.121 cm as the length in units and ρ is the dimensionless transverse direction in the range -200 to 200. We consider the strength of nonlocality as $\sigma = 10$. Fig. 10 and 11 shows the qualitative results of the numerical simulation showing the instability as the wave propagates along z direction.

V. CONCLUSION

We have theoretically studied the modulational instability of a composite system showing nonlocal nonlinear response. For our purpose, we have chosen the recent experimentally realized composite system of silver nanoparticles in acetone. Such system enable to realize a desired nonlinearity by properly choosing the volume fraction of the nanoparticles in the composite. This striking feature of such system is particularly attractive for nonlinear management. Taking advantage of this feature we have assumed different combinations of signs of nonlinearity, and systematically studied the dynamics of MI with particular emphasize on nonlocal nonlinearity. To generalize the impact of nonlocality, the commonly available form of nonlocal response functions have been considered. It is quite obvious from our study that the nonlocal response decreases the gain and bandwidth of MI, while at particular combination of the quintic nonlinearity it can even promotes new spectral bands. The rectangular response function is particularly attractive in MI dynamics, as it enables additional instability windows, whose width and numbers crucially depends on the strength of nonlocality. As far as cross coupling effects are concerned, the MI is typically enhanced by XPM and especially in the defocusing nonlinearity, the XPM effects are found to be fundamental to the origin of MI. The relative strength of

nonlinearity is another factor playing a substantial role either by increasing the gain or by promoting new spectral bands. We also noticed, the choice of the nonlocal response is indeed crucial, and the interplay with the nonlinearity accordingly impacts the MI dynamics. Thus we comprehensively studied the MI dynamics in the composite system with competing nonlinearities with a particular emphasize on nonlocal nonlinear response. As there are few works in the fabrication of composite systems, we believe our theoretical results could simulate new experiments especially in the context of nonlinear plasmonics.

Acknowledgments

K.P. thanks agencies DST, CSIR, NBHM, IFCPAR and DST-FCT, funded by the Government of India, for the financial support through major projects. KN acknowledges CNRS for post doctoral fellowship at the Université de Bourgogne, Dijon, and Agence Nationale de la Recherche (ANR) for the research fellowship at Université de Grenoble-Alpes, Grenoble, France.

References

-
- [1] N. Lepeshkin, W. Kim, V. Safonov, J. Zhu, R. Armstrong, C. White, R. Zuhr, and V. Shalaev, *Journal of Nonlinear Optical Physics and Materials* **8**, 191 (1999).
 - [2] X. Jiang, K. Guo, G. Liu, T. Yang, and Y. Yang, *Superlattices and Microstructures* **105**, 56 (2017).
 - [3] Y. Tsutsui, T. Hayakawa, G. Kawamura, and M. Nogami, *Nanotechnology* **22**, 275203 (2011).
 - [4] P. P. Kiran, B. N. S. Bhaktha, D. N. Rao, and G. De, *Journal of Applied Physics* **96**, 6717 (2004).
 - [5] Y. X. Zhang and Y. H. Wang, *RSC Advances* **7**, 45129 (2017).
 - [6] R. Souza, M. Alencar, E. Da Silva, M. Meneghetti, and J. Hickmann, *Appl. Phys. Lett.* **92**, 201902 (2008).
 - [7] A. Stalmashonak, G. Seifert, and A. Abdolvand, *Optical Properties of Nanocomposites Containing Metal Nanoparticles* (Springer International Publishing, Heidelberg, 2013), pp. 5–15.
 - [8] Z. A. V. Kauranen, Martti, *Nat Photon* **5**, 737748 (2012).
 - [9] A. S. Reyna, K. C. Jorge, and C. B. de Araújo, *Phys. Rev. A* **90**, 063835 (2014).
 - [10] A. Griesmaier, J. Stuhler, T. Koch, M. Fattori, T. Pfau, and S. Giovanazzi, *Phys. Rev. Lett.* **97**, 250402 (2006).
 - [11] M. Warenghem, J. F. Blach, and J. F. Henninot, *J. Opt. Soc. Am. B* **25**, 1882 (2008).
 - [12] V. M. Pérez-García, V. V. Konotop, and J. J. García-Ripoll, *Phys. Rev. E* **62**, 4300 (2000).
 - [13] J. F. Corney and O. Bang, *Phys. Rev. E* **64**, 047601 (2001).
 - [14] M. Warenghem, J. F. Blach, and J. F. Henninot, *J. Opt. Soc. Am. B* **25**, 1882 (2008).
 - [15] S. Skupin, M. Saffman, and W. Krukowski, *Phys. Rev. Lett.* **98**, 263902 (2007).
 - [16] Y. L. Zhou, Z. L. Zou, and K. Yan, *Water Science and Engineering* **5**, 419 (2012).
 - [17] M. Brunetti and J. Kasparian, *Phys. Lett. A* **378**, 3626 (2014).
 - [18] G. Murtaza and M. Salahuddin, *Plasma Physics* **24**, 451 (1982).
 - [19] O. Bouzit, M. Tribeche, and A. Bains, *Physics of Plasmas* **22**, 084506 (2015).
 - [20] G. Agrawal, *Nonlinear Fiber Optics* (Academic Press, 2013).
 - [21] V. Konotop and M. Salerno, *Phys. Rev. A* **65**, 021602/1 (2002).
 - [22] L. Li, Z. Li, B. Malomed, D. Mihalache, and W. Liu, *Phys. Rev. A* **72**, 033611 (2005).
 - [23] E. Wamba, A. Mohamadou, and T. Kofan, *Journ. of Phys. B* **41**, 225403 (2008).
 - [24] M. Peccianti, C. Conti, G. Assanto, A. DeLuca, and C. Umetsu, in *The 16th Annual Meeting of the IEEE Lasers and Electro-Optics Society, 2003. LEOS 2003.* (2003), vol. 1, pp. 31–32.
 - [25] T. P. Horikis, *Phys. Lett. A* **380**, 3473 (2016).
 - [26] J. Beeckman, X. Hutsebaut, M. Haelterman, and K. Neyts, *Opt. Express* **15**, 11185 (2007).
 - [27] R. Noskov, P. Belov, and Y. Kivshar, *Phys. Rev. Lett.* **108**, 093901 (2012).
 - [28] D. Korobko, S. Moiseev, and I. Zolotovskii, *Opt. Lett.* **40**, 4619 (2015).
 - [29] M. Kumar, K. Porsezian, P. Tchofo-Dinda, P. Grelu,

- T. Mithun, and T. Uthayakumar, *J. Opt. Soc. Am. B* **34**, 198 (2017).
- [30] K. Nithyanandan, R. Raja, T. Uthayakumar, and K. Porsezian, 2012 International Conference on Optical Engineering, ICOE 2012 p. 6409578 (2012).
- [31] M. Saha and A. K. Sarma, *Opt. Commun.* **291**, 321 (2013).
- [32] M. Saffman, G. McCarthy, and W. Krlikowski, *Jour.l of Opt. B: Quant. and Semic.l Opt.* **6**, S397 (2004).
- [33] E. O. Alves, W. B. Cardoso, and A. T. Avelar, *J. Opt. Soc. Am. B* **33**, 1134 (2016).
- [34] W. Krlikowski, O. Bang, N. I. Nikolov, D. Neshev, J. Wyller, J. J. Rasmussen, and D. Edmundson, *Journ. of Opt. B: Quant. and Semic.l Opt.* **6**, S288 (2004).
- [35] E. V. Doktorov and M. A. Molchan, *Proc. SPIE* **6725**, 6725 (2007).
- [36] A. S. Reyna and C. B. de Araújo, *Phys. Rev. A* **89**, 063803 (2014).
- [37] W. Krolikowski, O. Bang, J. J. Rasmussen, and J. Wyller, *Phys. Rev. E* **64**, 016612 (2001).
- [38] Z. Wang, Q. Guo, W. Hong, and W. Hu, *Optics Communications* **394**, 31 (2017).
- [39] C. L. Tiofack, H. Tagwo, O. Dafounansou, A. Mohamadou, and T. Kofane, *Opt. Comm.* **357**, 7 (2015).
- [40] H. Tagwo, C. Tiofack, O. Dafounansou, A. Mohamadou, and T. Kofane, *Journ.l of Mod. Opt.* **63**, 558 (2016).
- [41] G. Agrawal, *Phys. Rev. Lett* **59**, 880 (1987).
- [42] K. Nithyanandan, R. V. J. Raja, K. Porsezian, and B. Kalithasan, *Phys. Rev. A* **86**, 023827 (2012).
- [43] A. S. Reyna and C. B. de Araújo, *Opt. Express* **22**, 22456 (2014).
- [44] B. K. Esbensen, A. Wlotzka, M. Bache, O. Bang, and W. Krolikowski, *Phys. Rev. A* **84**, 053854 (2011).
- [45] J. Wyller, W. Krolikowski, O. Bang, and J. J. Rasmussen, *Phys. Rev. E* **66**, 066615 (2002).
- [46] Q. Kong, Q. Wang, O. Bang, and W. Krolikowski, *Opt. Lett.* **35**, 2152 (2010).